universe

MDPI

Article

Hadronic Molecules with Four Charm or Beauty Quarks

Wen-Ying Liu and Hua-Xing Chen *

School of Physics, Southeast University, Nanjing 210094, China
* Correspondence: hxchen@seu.edu.cn

Abstract: We apply extended local hidden-gauge formalism to study meson–meson interactions with the quark constituents $cc\bar{c}\bar{c}$, $cc\bar{c}\bar{b}/\bar{c}\bar{c}cb$, $cc\bar{b}\bar{b}/\bar{c}\bar{c}bb$, $bb\bar{c}\bar{b}/\bar{b}\bar{b}cb$, and $bb\bar{b}\bar{b}$, in which the exchanged mesons are the fully heavy vector mesons J/ψ, B_c^* and Υ. We solve the coupled-channel Bethe–Salpeter equation to derive two poles in the $bb\bar{c}\bar{b}$ system and two poles in the $cc\bar{c}\bar{b}$ system. There are also four charge-conjugated poles in the $\bar{b}\bar{b}cb$ and $\bar{c}\bar{c}cb$ systems. In the $bb\bar{c}\bar{b}$ system, one pole corresponds to a sub-threshold bound state when the cutoff momentum is set to $\Lambda > 850$ MeV. The other pole in this system corresponds to a sub-threshold bound state when $\Lambda > 1100$ MeV. In the $cc\bar{c}\bar{b}$ system, the two poles correspond to sub-threshold bound states only when $\Lambda > 1550$ MeV and $\Lambda > 2650$ MeV. This makes them difficult to identify as deeply bound hadronic molecules. We propose investigating the two poles of the $bb\bar{c}\bar{b}$ system in the $\mu^+\mu^-B_c^-$ channel at the LHC.

Keywords: fully heavy hadronic molecule; Bethe–Salpeter equation; local hidden-gauge formalism

1. Introduction

In recent decades, the study of exotic hadrons has gradually become a focal point in hadron physics. Some exotic hadrons exhibit multiquark compositions, such as the compact tetraquark states and the meson-meson molecular states [1–7]. The picture of hadronic molecules has achieved significant success in the light-quark sector [8–14], which can be used to explain many resonances, such as $f_0(980)$ and $a_0(980)$, etc. Additionally, many hidden-charm pentaquark states observed in the past decade can be interpreted as hadronic molecules that are dynamically generated through the meson–baryon interactions within the local hidden-gauge framework [15–22]. In recent years, several exotic structures in the di-J/ψ-invariant mass spectrum have been reported through the LHCb, CMS, and ATLAS collaborations [23–25], including $X(6200)$, $X(6600)$, $X(6900)$, and $X(7200)$. These structures are good candidates for fully charmed tetraquark states. Extensive theoretical investigations have been performed to elucidate their nature [26–68], some of which have attempted to explore their nature as molecular states [69–75], but a definitive and conclusive understanding of their nature remains elusive.

Previous theoretical studies on fully heavy tetraquark states mainly focus on the interpretation of compact tetraquark states, while there are not so many studies based on the interpretation of hadronic molecular states. This is because the exchanged hadrons of these systems have quite large masses, such as the fully heavy vector mesons J/ψ, B_c^*, and Υ exchanged in the $cb\bar{c}\bar{b}$ system within extended local hidden-gauge formalism, so their induced interactions are significantly suppressed. In Ref. [76], we studied the $cb\bar{c}\bar{b}$ system to explore the existence of fully heavy hadronic molecules $B_c^{(*)}\bar{B}_c^{(*)}$. Within the extended local hidden-gauge framework, we found that the two fully heavy mesons $B_c^{(*)}$ and $\bar{B}_c^{(*)}$ are able to form a bound state by exchanging the relatively lighter meson J/ψ.

check for updates

Academic Editor: Ignazio Bombaci

Received: 24 December 2024
Revised: 22 January 2025
Accepted: 23 January 2025
Published: 24 January 2025

Citation: Liu, W.-Y.; Chen, H.-X. Hadronic Molecules with Four Charm or Beauty Quarks. *Universe* **2025**, *11*, 36. https://doi.org/10.3390/universe11020036

Copyright: © 2025 by the authors. Licensee MDPI, Basel, Switzerland. This article is an open access article distributed under the terms and conditions of the Creative Commons Attribution (CC BY) license (https://creativecommons.org/licenses/by/4.0/).

In this paper, we apply extended local hidden-gauge formalism to further investigate the fully heavy hadronic molecules that exist in $cc\bar{c}\bar{c}$, $cc\bar{c}\bar{b}/\bar{c}\bar{c}cb$, $cc\bar{b}\bar{b}/\bar{c}\bar{c}bb$, $bb\bar{c}\bar{b}/\bar{b}\bar{b}cb$, and $bb\bar{b}\bar{b}$ systems. By solving the coupled-channel Bethe–Salpeter equation, we evaluate the hadronic molecules generated via the meson–meson interactions in these systems. Our results indicate the possible existence of two bound states in the $bb\bar{c}\bar{b}$ system, along with two charge-conjugated states in the $\bar{b}\bar{b}cb$ system. However, their manifestation depends on the cutoff momentum, as a result of which they may appear as threshold effects. Both structures share the same spin-parity quantum number $J^P = 1^+$, and they can potentially be observed in the $\mu^+\mu^- B_c^-$ channel at LHC. Additionally, we find two poles in the $cc\bar{c}\bar{b}$ system (with two charge-conjugated poles in the $\bar{c}\bar{c}cb$ system), but it is difficult to identify them as deeply bound hadronic molecules.

This paper is organized as follows. In Section 2, we apply local hidden-gauge formalism to derive the potentials for the interactions of the $cc\bar{c}\bar{c}$, $cc\bar{c}\bar{b}/\bar{c}\bar{c}cb$, $cc\bar{b}\bar{b}/\bar{c}\bar{c}bb$, $bb\bar{c}\bar{b}/\bar{b}\bar{b}cb$, and $bb\bar{b}\bar{b}$ systems. Based on the obtained results, we solve the coupled-channel Bethe–Salpeter equation in Section 3 to extract the poles, some of which may qualify as fully heavy hadronic molecules. A brief summary is provided in Section 4.

2. Formalism

In Ref. [76], we applied extended local hidden-gauge formalism to study the interactions of the $cb\bar{c}\bar{b}$ system. In this section, we follow the same approach to study the $cc\bar{c}\bar{c}$, $cc\bar{c}\bar{b}/\bar{c}\bar{c}cb$, $cc\bar{b}\bar{b}/\bar{c}\bar{c}bb$, $bb\bar{c}\bar{b}/\bar{b}\bar{b}cb$, and $bb\bar{b}\bar{b}$ systems. Note that the validity of extended local hidden-gauge formalism in these systems is still questionable. Within the framework of local hidden-gauge formalism [77,78], the vector mesons are considered to act as gauge bosons, transmitting interactions. This mechanism successfully describes many low-energy interactions [15,79–82], especially in processes dominated by the exchange of light vector mesons. Unfortunately, it is not clear whether this mechanism remains effective in the heavy flavor region. An extension of this method has also been developed to study molecular state candidates containing heavy quarks [15,20,83]. In these cases, generally, the exchange of light vector mesons and heavy vector mesons is allowed simultaneously. When the vector meson–vector meson interaction in the $c\bar{c}s\bar{s}$ system is taken as an example, this system involves two coupling channels: $D_s^*\bar{D}_s^*$ and $J/\psi\phi$. In the $D_s^*\bar{D}_s^*$ channel, the exchange of ϕ and J/ψ occurs simultaneously. Compared to the ϕ exchange, the J/ψ exchange is considered to be secondary due to its larger mass. However, things are somewhat different in the $J/\psi\phi$ channel. The minimal constituents for the exchanged meson should be $c\bar{c}s\bar{s}$, which we do not consider in local hidden-gauge formalism. Such a type of exchange mechanism should also be suppressed due to its involvement in the exchange of four quarks. On the other hand, the $J/\psi\phi$ channel can couple with the $D_s^*\bar{D}_s^*$ channel, which allows for the exchange of the heavy vector meson D_s^* between these two channels. Although the exchange of heavy vector mesons should be relatively minimal, it plays a role in this scenario. Under this assumption, results consistent with experiments can be obtained [83]. So, the present study, as well as Ref. [76], serve as pioneering research investigating fully heavy hadronic molecules. Within this framework, the interactions are primarily contributed via the vector meson exchange, as depicted in Figure 1. The corresponding Lagrangians are written as follows:

$$
\begin{aligned}
\mathcal{L}_{VPP} &= -ig\,\langle [P, \partial_\mu P] V^\mu \rangle\,, \\
\mathcal{L}_{VVV} &= ig\,\langle (V^\mu \partial_\nu V_\mu - \partial_\nu V^\mu V_\mu) V^\nu \rangle\,, \\
\mathcal{L}_{VVVV} &= \frac{g^2}{2}\langle V_\mu V_\nu V^\mu V^\nu - V_\nu V_\mu V^\mu V^\nu \rangle\,,
\end{aligned}
\tag{1}
$$

where

$$P = \begin{pmatrix} \eta_c & B_c^+ \\ B_c^- & \eta_b \end{pmatrix}, \quad V = \begin{pmatrix} J/\psi & B_c^{*+} \\ B_c^{*-} & \Upsilon \end{pmatrix}. \tag{2}$$

The coupling constant g is generally defined as $g = M_V/(2f_P)$, with M_V being the mass of the exchanged vector meson and f_P being the decay constant of its corresponding pseudoscalar meson. Since the charm and bottom quarks do not form a flavor symmetry, $SU(2)$, we cannot use an overall parameter. For the exchange of the J/ψ, B_c^*, and Υ mesons, we respectively use $M_{J/\psi} = 3096.9$ MeV [84], $f_{\eta_c} = 387/\sqrt{2}$ MeV [85], $M_{B_c^*} = 6331$ MeV [86], $f_{B_c} = 427/\sqrt{2}$ MeV [87], $M_\Upsilon = 9460.4$ MeV [84], $f_{\eta_b} = 667/\sqrt{2}$ MeV [87]. Additionally, we use $g^4 = g_{V_1}g_{V_2}g_{V_3}g_{V_4}$ for the contact term, with $V_{1\cdots4}$ denoting the four connected vector mesons.

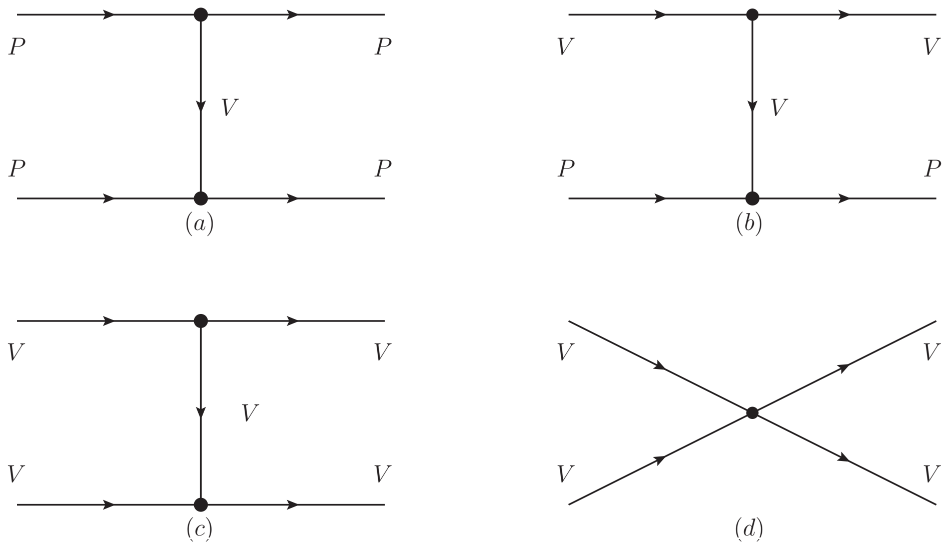

Figure 1. The meson–meson interactions arising from the vector meson exchange: (**a**) between two pseudoscalar mesons, (**b**) between one vector meson and one pseudoscalar meson, and (**c**) between two vector mesons. The subfigure (**d**) describes the contact term connecting four vector mesons.

We derive the following interaction potential from the Lagrangians given in Equation (1):

$$\begin{aligned} V_{PP}(s) &= C_{PP}^t \times g^2(p_1+p_3)(p_2+p_4) \\ &+ C_{PP}^u \times g^2(p_1+p_4)(p_2+p_3), \end{aligned} \tag{3}$$

$$\begin{aligned} V_{VP}(s) &= C_{VP}^t \times g^2(p_1+p_3)(p_2+p_4)\,\epsilon_1\cdot\epsilon_3 \\ &+ C_{VP}^u \times g^2(p_1+p_4)(p_2+p_3)\,\epsilon_1\cdot\epsilon_3, \end{aligned} \tag{4}$$

$$V_{VV}(s) = V_{VV}^{ex}(s) + V_{VV}^{co}(s), \tag{5}$$

$$\begin{aligned} V_{VV}^{ex}(s) &= C_{VV}^t \times g^2(p_1+p_3)(p_2+p_4)\epsilon_1\cdot\epsilon_3\epsilon_2\cdot\epsilon_4 \\ &+ C_{VV}^u \times g^2(p_1+p_3)(p_2+p_4)\epsilon_1\cdot\epsilon_4\epsilon_2\cdot\epsilon_3, \end{aligned} \tag{6}$$

where p_1 and p_2 are four-momenta of the incoming mesons, p_3 and p_4 are four-momenta of the outgoing mesons, ϵ_1 and ϵ_2 are polarization vectors of the incoming mesons, and ϵ_3 and ϵ_4 are polarization vectors of the outgoing mesons. We use the subscripts PP, VP, and VV to denote the pseudoscalar–pseudoscalar, vector–pseudoscalar, and vector–vector sectors, respectively. We use the superscripts t, u, and co to denote the vector meson exchange in the t and u channels, as well as the contact term, respectively. Note that the coefficient C_{VP}^u is zero because we only consider the vector meson exchange in the present study. Actually, there also exists the pseudoscalar meson exchange. As evaluated in detail in Refs. [88,89], the contribution of the pseudoscalar meson exchange is negligible near the threshold compared to the vector meson exchange. This is because the amplitude of the vector meson exchange is proportional to the energy of the external meson, while the amplitude of the pseudoscalar meson exchange is proportional to the three-momentum of the external meson, which is always negligible near the threshold.

We further derive the scattering amplitudes from Equations (3)–(6) by solving the Bethe–Salpeter equation as

$$T_{PP/VP/VV} = (\mathbf{1} - V_{PP/VP/VV} \bullet G)^{-1} \bullet V_{PP/VP/VV}, \tag{7}$$

where $G(s)$ is the diagonal loop function, whose expression for the ith channel is

$$G_{ii}(s) = i \int \frac{d^4q}{(2\pi)^4} \frac{1}{q^2 - m_1^2 + i\epsilon} \frac{1}{(p-q)^2 - m_2^2 + i\epsilon} . \tag{8}$$

In the above expression, $m_{1,2}$ are the masses of the two mesons involved in this channel, and $s = p^2$ with p is the total four-momentum. We apply the cutoff method to regularize it as

$$G_{ii}(s) = \int_0^\Lambda \frac{d^3q}{(2\pi)^3} \frac{\omega_1 + \omega_2}{2\omega_1\omega_2} \frac{1}{s - (\omega_1 + \omega_2)^2 + i\epsilon} , \tag{9}$$

where $\omega_1 = \sqrt{m_1^2 + \vec{q}^{\,2}}$, $\omega_2 = \sqrt{m_2^2 + \vec{q}^{\,2}}$, and Λ is the cutoff momentum.

We shall calculate the coefficient matrices $C^{t/u/co}_{PP/VP/VV}$ in the following subsections separately for the $cc\bar{c}\bar{c}$, $cc\bar{c}\bar{b}/\bar{c}\bar{c}cb$, $cc\bar{b}\bar{b}/\bar{c}\bar{c}bb$, $bb\bar{c}\bar{b}/\bar{b}\bar{b}cb$, and $bb\bar{b}\bar{b}$ systems. Before doing this, we summarize their relevant coupled channels in Table 1.

Table 1. Coupled channels considered for the $cc\bar{c}\bar{c}$, $cc\bar{c}\bar{b}/\bar{c}\bar{c}cb$, $cc\bar{b}\bar{b}/\bar{c}\bar{c}bb$, $bb\bar{c}\bar{b}/\bar{b}\bar{b}cb$, and $bb\bar{b}\bar{b}$ systems.

Constituent	*PP* Sector	*VP* Sector	*VV* Sector
$cc\bar{c}\bar{c}$	$\eta_c\eta_c$	$J/\psi\eta_c$	$J/\psi J/\psi$
$cc\bar{c}\bar{b}$	$\eta_c B_c^+$	$J/\psi B_c^+$, $B_c^{*+}\eta_c$	$J/\psi B_c^{*+}$
$cc\bar{b}\bar{b}$	$B_c^+ B_c^+$	$B_c^{*+} B_c^+$	$B_c^{*+} B_c^{*+}$
$bb\bar{c}\bar{b}$	$\eta_b B_c^-$	ΥB_c^-, $B_c^{*-}\eta_b$	ΥB_c^{*-}
$bb\bar{b}\bar{b}$	$\eta_b\eta_b$	$\Upsilon\eta_b$	$\Upsilon\Upsilon$

2.1. The $cc\bar{c}\bar{c}$ System

In the $cc\bar{c}\bar{c}$ system, the PP interaction involves only one channel, $\eta_c\eta_c$, the VP interaction involves only one channel, $J/\psi\eta_c$, and the VV interaction also involves only one channel, $J/\psi J/\psi$. Additionally, the $bb\bar{b}\bar{b}$ system can be similarly investigated.

Since the two vertices are both zero, $\mathcal{L}_{\eta_c\eta_c J/\psi} = 0$ and $\mathcal{L}_{J/\psi J/\psi J/\psi} = 0$, the interactions in this system all vanish within the extended local hidden-gauge framework:

$$\begin{aligned} C^t_{PP} &= C^u_{PP} = 0\,, \\ C^t_{VP} &= C^u_{VP} = 0\,, \\ C^t_{VV} &= C^u_{VV} = 0\,, \\ C^{co}_{VV} &= 0\,. \end{aligned} \tag{10}$$

The $bb\bar{b}\bar{b}$ system and the $cc\bar{c}\bar{c}$ system exhibit very similar dynamic properties, with the only distinction being their mass differences. Consequently, they share the same coefficients listed in Equation (10), implying that the interactions within the $bb\bar{b}\bar{b}$ system also vanish.

Therefore, our results do not support the existence of hadronic molecules in the $cc\bar{c}\bar{c}$ and $bb\bar{b}\bar{b}$ systems. Moreover, our conclusions do not actually depend on the value of the coupling constant g. As long as the near-threshold interactions in these systems are dominated by vector meson exchange and can be described by the Lagrangian in Equation (1), the validity of the conclusions can be maintained. Let us examine the specific form of the t-channel exchange potential in Equation (3):

$$-iV^t = ig_1(p_1+p_3)^\mu ig_2(p_2+p_4)^\nu \frac{i(-g_{\mu\nu}+\frac{q_\mu q_\nu}{m_V^2})}{t-m_V^2}\,, \tag{11}$$

where p_1 and p_2 are four-momenta of the incoming mesons, p_3 and p_4 are four-momenta of the outgoing mesons, q is a four-momentum of the exchanged meson and g_1 and g_2 are two coupling constants corresponding to the top and bottom vertices in Figure 1a. When the three-momenta of the particles are ignored and t is approximated as 0, the following simplification can be obtained:

$$V^t \simeq \frac{g_1 g_2}{m_V^2}(m_1+m_3)\cdot(m_2+m_4). \tag{12}$$

It can be found that, if the particles in the channels are identical, i.e., $g_1 = g_2$, the interaction will be repulsive. Similar derivations also apply to the exchange potential V^u in the u-channel. This indicates that the existence of near-threshold molecular states in channels similar to $\eta_c\eta_c$ is difficult to support. The experimentally observed states in these systems are, therefore, good candidates to be tetraquark states.

2.2. The $cc\bar{c}\bar{b}$ and $\bar{c}\bar{c}cb$ Systems

The results for the $cc\bar{c}\bar{b}$ and $\bar{c}\bar{c}cb$ systems are the same, so we only need to study the $cc\bar{c}\bar{b}$ system. Additionally, the $bb\bar{c}\bar{b}$ and $\bar{b}\bar{b}cb$ systems can be similarly investigated. In the $cc\bar{c}\bar{b}$ system, the PP interaction involves only one channel, $\eta_c B_c^+$, whose coefficients are

$$\begin{aligned} C^t_{PP} &= 0\,, \\ C^u_{PP} &= \lambda\frac{1}{m^2_{B_c^*}}\,. \end{aligned} \tag{13}$$

The reduction factor λ existing in the u channel, is introduced to account for the large mass difference between the initial meson η_c and the final meson B_c^+ (or between the initial meson B_c^+ and the final meson η_c). Following Ref. [90], numerically, we use

$$\lambda_{\eta_c B_c^+\to B_c^+\eta_c} \approx \frac{-m^2_{B_c^*}}{(m_{\eta_c}-m_{B_c})^2 - m^2_{B_c^*}} = 1.37. \tag{14}$$

The coefficient C^u_{PP} is positive, indicating that the interaction due to the exchange of the B_c^* meson is repulsive; hence, hadronic molecules in the PP sector are not expected to exist.

The VP interaction involves two coupled channels, $J/\psi B_c^+$ and $B_c^{*+}\eta_c$, whose coefficients are

$$\begin{aligned} C^t_{VP} &= \left(\begin{array}{c|cc} J=1 & J/\psi B_c^+ & B_c^{*+}\eta_c \\ \hline J/\psi B_c^+ & 0 & \lambda\frac{1}{m^2_{B_c^*}} \\ B_c^{*+}\eta_c & \lambda\frac{1}{m^2_{B_c^*}} & 0 \end{array}\right) \quad \textit{and} \\ C^u_{VP} &= \mathbf{0}_{2\times 2}\,. \end{aligned} \tag{15}$$

Diagonalizing this 2×2 matrix, we obtain two decoupled channels:

$$|VP^+\rangle = \frac{1}{\sqrt{2}}\big(|J/\psi B_c^+\rangle + |B_c^{*+}\eta_c\rangle\big), \tag{16}$$

$$|VP^-\rangle = \frac{1}{\sqrt{2}}\big(|J/\psi B_c^+\rangle - |B_c^{*+}\eta_c\rangle\big), \tag{17}$$

whose coefficient is

$$C'^t_{VP} = \left(\begin{array}{c|cc} J=1 & VP^+ & VP^- \\ \hline VP^+ & \lambda\frac{1}{m^2_{B_c^*}} & 0 \\ VP^- & 0 & -\lambda\frac{1}{m^2_{B_c^*}} \end{array}\right). \tag{18}$$

Hence, the interaction due to the exchange of the B_c^* meson in the VP^- channel turns out to be attractive, so there may exist a hadronic molecule of $J^P = 1^+$ in the VP sector.

The VV interaction involves only one channel, $J/\psi B_c^{*+}$, whose coefficients are

$$C^t_{VV} = 0 \quad and \qquad C^u_{VV} = \lambda\frac{1}{m^2_{B_c^*}}\,. \tag{19}$$

The relevant contact term is

$$V^{co}_{J/\psi B_c^{*+}\to J/\psi B_c^{*+}}(s) = \begin{cases} -2g^2 & \text{for } J=0, \\ 3g^2 & \text{for } J=1, \\ g^2 & \text{for } J=2. \end{cases} \tag{20}$$

After performing the spin projection, we find the $J = 1$ channel to be attractive, so there may exist a hadronic molecule of $J^P = 1^+$ in the VV sector.

2.3. The $cc\bar{b}\bar{b}$ and $\bar{c}\bar{c}bb$ Systems

The results for the $cc\bar{b}\bar{b}$ and $\bar{c}\bar{c}bb$ systems are the same, so we only need to study the $cc\bar{b}\bar{b}$ system. In this system, the PP interaction involves only one channel, $B_c^+B_c^+$, whose coefficients are

$$C^t_{PP} = \frac{1}{m^2_{J/\psi}} + \frac{1}{m^2_{\Upsilon}} \quad and \qquad C^u_{PP} = \frac{1}{m^2_{J/\psi}} + \frac{1}{m^2_{\Upsilon}}\,. \tag{21}$$

The VP interaction involves only one channel, $B_c^{*+}B_c^+$, whose coefficient are

$$C^t_{VP} = \frac{1}{m^2_{J/\psi}} + \frac{1}{m^2_{\Upsilon}} \quad and \qquad C^u_{VP} = 0\,. \tag{22}$$

The VV interaction also involves only one channel, $B_c^{*+}B_c^{*+}$, whose coefficients are

$$C^t_{VV} = \frac{1}{m^2_{J/\psi}} + \frac{1}{m^2_{\Upsilon}} \quad and \qquad C^u_{VV} = \frac{1}{m^2_{J/\psi}} + \frac{1}{m^2_{\Upsilon}}\,. \tag{23}$$

The relevant contact term is

$$V^{co}_{B_c^{*+}B_c^{*+}\to B_c^{*+}B_c^{*+}}(s) = \begin{cases} -8g^2 & \text{for } J=0, \\ 0 & \text{for } J=1, \\ 4g^2 & \text{for } J=2. \end{cases} \tag{24}$$

In sectors other than the $|(VV)_{cc\bar{b}\bar{b}}; J^P = 0^+\rangle$ sector, the coefficients are positive, corresponding to repulsive interactions. As for the $|(VV)_{cc\bar{b}\bar{b}}; J^P = 0^+\rangle$ sector, although the contact term provides an attractive potential of $-8g^2$, the repulsive potential generated via the exchange of vector mesons is approximately $+13g^2$ at the threshold, resulting in an overall repulsive interaction. Therefore, in these sectors, the exchange of vector mesons cannot bind mesons together; hence, the above coefficients do not support the existence of hadronic molecules in the $cc\bar{b}\bar{b}$ system.

3. Numerical Results

In the previous section, we studied the interactions of the $cc\bar{c}\bar{c}$, $cc\bar{c}\bar{b}/\bar{c}\bar{c}cb$, $cc\bar{b}\bar{b}/\bar{c}\bar{c}bb$, $bb\bar{c}\bar{b}/\bar{b}\bar{b}cb$, and $bb\bar{b}\bar{b}$ systems. In this section, we numerically study their properties. As shown in Equation (9), the loop function $G(s)$ is regularized using the cutoff method, with the cutoff momentum Λ describing the dynamical scale to be integrated out. Its value is quite uncertain for the exchange of fully heavy vector mesons, and we follow Ref. [76] in choosing a broad region, $\Lambda = 400 \sim 1400$ MeV, to perform numerical analyses, since the authors of Refs. [91,92] have already found that the requirement of heavy quark symmetry demands the use of the same cutoff momentum in the charm and bottom sectors. We note that the value of this important parameter is quite uncertain for the exchange of fully heavy vector mesons, so the present study, as well as Ref. [76], serves as pioneering research investigating the fully heavy hadronic molecules, but there do exist large theoretical uncertainties.

Within the extended local hidden-gauge framework, the resonances are dynamically generated as poles of the scattering amplitudes $T_{PP/VP/VV}(s)$. We find the existence of eight poles that may lead to some singular structures on the invariant mass spectrum. There exist two poles in the $cc\bar{c}\bar{b}$ system and two poles in the $bb\bar{c}\bar{b}$ system, which we shall discuss in detail later. We summarize their positions in Table 2 with respect to the cutoff momentum Λ. Additionally, there exist four charge-conjugated poles in the $\bar{c}\bar{c}cb$ and $\bar{b}\bar{b}cb$ systems.

Table 2. Pole positions with respect to the cutoff momentum Λ in units of MeV. We only list the poles that correspond to the sub-threshold bound states.

	$\Lambda = 400$	$\Lambda = 600$	$\Lambda = 800$	$\Lambda = 1000$	$\Lambda = 1200$	$\Lambda = 1400$
$\|(VP)_{cc\bar{c}\bar{b}}; J^P = 1^+\rangle$	$--$	$--$	$--$	$--$	$--$	$--$
$\|(VV)_{cc\bar{c}\bar{b}}; J^P = 1^+\rangle$	$--$	$--$	$--$	$--$	$--$	$--$
$\|(VP)_{bb\bar{c}\bar{b}}; J^P = 1^+\rangle$	$--$	$--$	$--$	$15{,}725.3 - i0$	$15{,}710.8 - i0$	$15{,}685.2 - i0$
$\|(VV)_{bb\bar{c}\bar{b}}; J^P = 1^+\rangle$	$--$	$--$	$--$	$--$	$15{,}790.3 - i0$	$15{,}784.0 - i0$

We find two poles in the $cc\bar{c}\bar{b}$ system: one pole in the VP sector and the other in the VV sector. However, both of them correspond to virtual states when the cutoff momentum is set to $\Lambda = 400 \sim 1400$ MeV, so they can only result in some threshold effects. The pole in the VP sector corresponds to the sub-threshold bound state with $\Lambda > 1550$ MeV, and the pole in the VV sector corresponds to the sub-threshold bound state with $\Lambda > 2650$ MeV. We generally consider the cutoff momentum Λ to be consistent with the chiral unitary approach, which takes $\Lambda \approx 4\pi f_\pi \simeq 1200$ MeV. This value reflects certain non-perturbative properties of QCD. However, it is important to note that the parameter Λ also functions as a free parameter, absorbing some implicitly considered interactions, and as a result, it may deviate from 1200 MeV in practical applications. Empirically, Λ is usually taken to fall within the range of 400 to 700 MeV. Given the uncertainties inherent to our work, we believe it is appropriate to extend this range to 400 to 1400 MeV. Therefore, our results do not support the existence of deeply bound hadronic molecules in the $cc\bar{c}\bar{b}$ system.

We also find two poles in the $bb\bar{c}\bar{b}$ system: one pole in the VP sector and the other in the VV sector. The pole in the VP sector corresponds to the sub-threshold bound state when $\Lambda > 850$ MeV is set, making it possible to be identified as a hadronic molecule. This pole transfers to a virtual state and results in the threshold effect when $\Lambda < 850$ MeV is set. The pole in the VV sector corresponds to the sub-threshold bound state with $\Lambda > 1100$ MeV. To illustrate these two poles, we present, in Figure 2, the transition amplitudes using several different values of the cutoff momentum Λ.

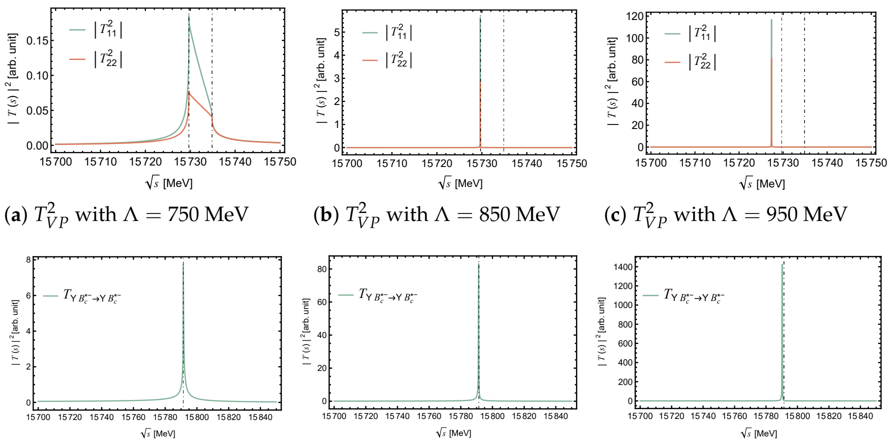

(**a**) T^2_{VP} with $\Lambda = 750$ MeV (**b**) T^2_{VP} with $\Lambda = 850$ MeV (**c**) T^2_{VP} with $\Lambda = 950$ MeV

(**d**) T^2_{VV} with $\Lambda = 1000$ MeV (**e**) T^2_{VV} with $\Lambda = 1100$ MeV (**f**) T^2_{VV} with $\Lambda = 1200$ MeV

Figure 2. Line shapes of the transition amplitudes $|T(s)|^2$ for the cutoff momentum $\Lambda =$ (**a**) 750 MeV, (**b**) 850 MeV, and (**c**) 950 MeV in the VP sector, as well as $\Lambda =$ (**d**) 1000 MeV, (**e**) 1100 MeV, and (**f**) 1200 MeV in the $VV|_{J=1}$ sector of the $bb\bar{c}\bar{b}$ system. The relevant thresholds are indicated by dashed lines. In subfigures (**a**–**c**), the green line labeled T_{11} and the red line labeled T_{22} represent $|T_{\Upsilon B_c^- \to \Upsilon B_c^-}(s)|^2$ and $|T_{B_c^{*-}\eta_b \to B_c^{*-}\eta_b}(s)|^2$, respectively.

4. Conclusions

In this paper, we have studied fully heavy meson–meson interactions with the quark constituents $cc\bar{c}\bar{c}$, $cc\bar{c}\bar{b}/\bar{c}\bar{c}cb$, $cc\bar{b}\bar{b}/\bar{c}\bar{c}bb$, $bb\bar{c}\bar{b}/\bar{b}\bar{b}cb$, and $bb\bar{b}\bar{b}$ through extended local hidden-gauge formalism. After solving the coupled-channel Bethe–Salpeter equation, we searched for poles on both the first (physical) and second Riemann sheets. The obtained results are summarized in Table 2 with respect to the cutoff momentum Λ. We found two poles in the $bb\bar{c}\bar{b}$ system (and two charge-conjugated poles in the $\bar{b}\bar{b}cb$ system): the pole generated in the VP sector corresponds to the sub-threshold bound state when the cutoff momentum $\Lambda > 850$ MeV is set, and the pole generated in the VV sector corresponds to the sub-threshold bound state with $\Lambda > 1100$ MeV. These two poles are potential fully heavy hadronic molecules, and we propose to investigate them in the $\mu^+\mu^- B_c^-$ channel at LHC. However, our results do not support the existence of hadronic molecules in the $cc\bar{c}\bar{c}$, $cc\bar{c}\bar{b}/\bar{c}\bar{c}cb$, $cc\bar{b}\bar{b}/\bar{c}\bar{c}bb$, and $bb\bar{b}\bar{b}$ systems.

Additionally, the $cb\bar{c}\bar{b}$ system has already been investigated in our previous study [76], where we found the existence of the fully heavy hadronic molecules $|B_c^+ B_c^-; J^{PC} = 0^{++}\rangle$, $|B_c^{*+} B_c^- - c.c.; J^{PC} = 1^{+-}\rangle$, and $|B_c^{*+} B_c^{*-}; J^{PC} = 2^{++}\rangle$, as well as the possible existence of $|B_c^{*+} B_c^- + c.c.; J^{PC} = 1^{++}\rangle$. We further proposed in Ref. [76] that a lower-mass fully heavy meson may be able to bind two higher-mass fully heavy hadrons. The results obtained in the present study are consistent with this proposal: the exchanged mesons of the $bb\bar{c}\bar{b}$ and $cc\bar{c}\bar{b}$ systems are both the B_c^* meson, but the larger mass of the $bb\bar{c}\bar{b}$ system facilitates the formation of bound states. It is a topic of considerable interest whether the interaction of the heavy meson exchange is strong enough to form hadronic molecules. This question serves as a crucial test for the extensively investigated interaction of the light meson exchange. Therefore, the present study, as well as Ref. [76], both of which concentrate on the interaction of the fully heavy meson exchange, are of particular interest.

Author Contributions: Conceptualization, W.-Y.L. and H.-X.C.; methodology, W.-Y.L. and H.-X.C.; software, W.-Y.L.; validation, W.-Y.L.; formal analysis, W.-Y.L.; investigation, W.-Y.L.; resources, W.-Y.L.; data curation, W.-Y.L.; writing—original draft preparation, W.-Y.L. and H.-X.C.; writing—review and editing, W.-Y.L. and H.-X.C.; visualization, W.-Y.L.; supervision, H.-X.C.; project administration, H.-X.C.; funding acquisition, H.-X.C. All authors have read and agreed to the published version of the manuscript.

Funding: This project is supported by the National Natural Science Foundation of China under Grant No. 12075019, the Jiangsu Provincial Double-Innovation Program under Grant No. JSSCRC2021488, and the Fundamental Research Funds for the Central Universities.

Data Availability Statement: No new data were created or analyzed in this study.

Conflicts of Interest: The authors declare no conflicts of interest.

References

1. Liu, Y.R.; Chen, H.X.; Chen, W.; Liu, X.; Zhu, S.L. Pentaquark and Tetraquark States. *Prog. Part. Nucl. Phys.* **2019**, *107*, 237–320. https://doi.org/10.1016/j.ppnp.2019.04.003.
2. Chen, H.X.; Chen, W.; Liu, X.; Liu, Y.R.; Zhu, S.L. An updated review of the new hadron states. *Rept. Prog. Phys.* **2023**, *86*, 026201. https://doi.org/10.1088/1361-6633/aca3b6.
3. Guo, F.K.; Hanhart, C.; Meißner, U.G.; Wang, Q.; Zhao, Q.; Zou, B.S. Hadronic molecules. *Rev. Mod. Phys.* **2018**, *90*, 015004. https://doi.org/10.1103/RevModPhys.90.015004.
4. Brambilla, N.; Eidelman, S.; Hanhart, C.; Nefediev, A.; Shen, C.P.; Thomas, C.E.; Vairo, A.; Yuan, C.Z. The *XYZ* states: Experimental and theoretical status and perspectives. *Phys. Rept.* **2020**, *873*, 1–154. https://doi.org/10.1016/j.physrep.2020.05.001.
5. Esposito, A.; Pilloni, A.; Polosa, A.D. Multiquark resonances. *Phys. Rept.* **2017**, *668*, 1–97. https://doi.org/10.1016/j.physrep.2016.11.002.
6. Lebed, R.F.; Mitchell, R.E.; Swanson, E.S. Heavy-quark QCD exotica. *Prog. Part. Nucl. Phys.* **2017**, *93*, 143–194. https://doi.org/10.1016/j.ppnp.2016.11.003.
7. Ali, A.; Lange, J.S.; Stone, S. Exotics: Heavy pentaquarks and tetraquarks. *Prog. Part. Nucl. Phys.* **2017**, *97*, 123–198. https://doi.org/10.1016/j.ppnp.2017.08.003.
8. Oller, J.A.; Oset, E. Chiral symmetry amplitudes in the S wave isoscalar and isovector channels and the σ, $f_0(980)$, $a_0(980)$ scalar mesons. *Nucl. Phys. A* **1997**, *620*, 438–456. https://doi.org/10.1016/S0375-9474(97)00160-7.
9. Oller, J.A.; Oset, E.; Pelaez, J.R. Meson meson interaction in a nonperturbative chiral approach. *Phys. Rev. D* **1999**, *59*, 074001. Erratum: *Phys .Rev. D* **1999**, *60*, 099906; Erratum: *Phys. Rev. D* **2007**, *75*, 099903. https://doi.org/10.1103/PhysRevD.59.074001.
10. Oset, E.; Ramos, A. Nonperturbative chiral approach to s wave anti-K N interactions. *Nucl. Phys. A* **1998**, *635*, 99–120. https://doi.org/10.1016/S0375-9474(98)00170-5.
11. Jido, D.; Oller, J.A.; Oset, E.; Ramos, A.; Meissner, U.G. Chiral dynamics of the two Lambda(1405) states. *Nucl. Phys. A* **2003**, *725*, 181–200. https://doi.org/10.1016/S0375-9474(03)01598-7.
12. Bruns, P.C.; Mai, M.; Meissner, U.G. Chiral dynamics of the S11(1535) and S11(1650) resonances revisited. *Phys. Lett. B* **2011**, *697*, 254–259. https://doi.org/10.1016/j.physletb.2011.02.008.
13. Garcia-Recio, C.; Lutz, M.F.M.; Nieves, J. Quark mass dependence of s wave baryon resonances. *Phys. Lett. B* **2004**, *582*, 49–54. https://doi.org/10.1016/j.physletb.2003.11.073.

14. Hyodo, T.; Nam, S.I.; Jido, D.; Hosaka, A. Flavor SU(3) breaking effects in the chiral unitary model for meson baryon scatterings. *Phys. Rev. C* **2003**, *68*, 018201. https://doi.org/10.1103/PhysRevC.68.018201.
15. Wu, J.J.; Molina, R.; Oset, E.; Zou, B.S. Prediction of Narrow N^* and Λ^* Resonances with Hidden Charm above 4 GeV. *Phys. Rev. Lett.* **2010**, *105*, 232001. https://doi.org/10.1103/PhysRevLett.105.232001.
16. Wu, J.J.; Molina, R.; Oset, E.; Zou, B.S. Dynamically generated N^* and Λ^* resonances in the hidden charm sector around 4.3 GeV. *Phys. Rev. C* **2011**, *84*, 015202. https://doi.org/10.1103/PhysRevC.84.015202.
17. Chen, H.X.; Geng, L.S.; Liang, W.H.; Oset, E.; Wang, E.; Xie, J.J. Looking for a hidden-charm pentaquark state with strangeness $S = -1$ from Ξ_b^- decay into $J/\psi K^- \Lambda$. *Phys. Rev. C* **2016**, *93*, 065203. https://doi.org/10.1103/PhysRevC.93.065203.
18. He, J. $\bar{D}\Sigma_c^*$ and $\bar{D}^*\Sigma_c$ interactions and the LHCb hidden-charmed pentaquarks. *Phys. Lett. B* **2016**, *753*, 547–551. https://doi.org/10.1016/j.physletb.2015.12.071.
19. Xiao, C.W.; Nieves, J.; Oset, E. Combining heavy quark spin and local hidden gauge symmetries in the dynamical generation of hidden charm baryons. *Phys. Rev. D* **2013**, *88*, 056012. https://doi.org/10.1103/PhysRevD.88.056012.
20. Roca, L.; Nieves, J.; Oset, E. LHCb pentaquark as a $\bar{D}^*\Sigma_c - \bar{D}^*\Sigma_c^*$ molecular state. *Phys. Rev. D* **2015**, *92*, 094003. https://doi.org/10.1103/PhysRevD.92.094003.
21. Liu, X.H.; Wang, Q.; Zhao, Q. Understanding the newly observed heavy pentaquark candidates. *Phys. Lett. B* **2016**, *757*, 231–236. https://doi.org/10.1016/j.physletb.2016.03.089.
22. Uchino, T.; Liang, W.H.; Oset, E. Baryon states with hidden charm in the extended local hidden gauge approach. *Eur. Phys. J. A* **2016**, *52*, 43. https://doi.org/10.1140/epja/i2016-16043-0.
23. Aaij, R. et al. [LHCb Collaboration]. Observation of structure in the J/ψ -pair mass spectrum. *Sci. Bull.* **2020**, *65*, 1983–1993. https://doi.org/10.1016/j.scib.2020.08.032.
24. Aad, G. et al. [ATLAS Collaboration]. Observation of an Excess of Dicharmonium Events in the Four-Muon Final State with the ATLAS Detector. *Phys. Rev. Lett.* **2023**, *131*, 151902. https://doi.org/10.1103/PhysRevLett.131.151902.
25. Hayrapetyan, A. et al. [CMS Collaboration]. Observation of new structure in the J/ψJ/ψ mass spectrum in proton-proton collisions at $\sqrt{s}$ = 13 TeV *arXiv* **2023**, arXiv:hep-ex/2306.07164.
26. Liu, M.S.; Liu, F.X.; Zhong, X.H.; Zhao, Q. Full-heavy tetraquark states and their evidences in the LHCb di-J/ψ spectrum. *arXiv* **2020**, arXiv:hep-ph/2006.11952.
27. Tiwari, R.; Rathaud, D.P.; Rai, A.K. Spectroscopy of all charm tetraquark states. *arXiv* **2021**, arXiv:hep-ph/2108.04017.
28. Lü, Q.F.; Chen, D.Y.; Dong, Y.B. Masses of fully heavy tetraquarks $QQ\bar{Q}\bar{Q}$ in an extended relativized quark model. *Eur. Phys. J. C* **2020**, *80*, 871. https://doi.org/10.1140/epjc/s10052-020-08454-1.
29. Faustov, R.N.; Galkin, V.O.; Savchenko, E.M. Masses of the $QQ\bar{Q}\bar{Q}$ tetraquarks in the relativistic diquark-antidiquark picture. *Phys. Rev. D* **2020**, *102*, 114030. https://doi.org/10.1103/PhysRevD.102.114030.
30. Zhang, J.R. 0^+ fully-charmed tetraquark states. *Phys. Rev. D* **2021**, *103*, 014018. https://doi.org/10.1103/PhysRevD.103.014018.
31. Li, Q.; Chang, C.H.; Wang, G.L.; Wang, T. Mass spectra and wave functions of $T_{QQ\bar{Q}\bar{Q}}$ tetraquarks. *Phys. Rev. D* **2021**, *104*, 014018. https://doi.org/10.1103/PhysRevD.104.014018.
32. Bedolla, M.A.; Ferretti, J.; Roberts, C.D.; Santopinto, E. Spectrum of fully-heavy tetraquarks from a diquark+antidiquark perspective. *Eur. Phys. J. C* **2020**, *80*, 1004. https://doi.org/10.1140/epjc/s10052-020-08579-3.
33. Weng, X.Z.; Chen, X.L.; Deng, W.Z.; Zhu, S.L. Systematics of fully heavy tetraquarks. *Phys. Rev. D* **2021**, *103*, 034001. https://doi.org/10.1103/PhysRevD.103.034001.
34. Liu, F.X.; Liu, M.S.; Zhong, X.H.; Zhao, Q. Higher mass spectra of the fully-charmed and fully-bottom tetraquarks. *Phys. Rev. D* **2021**, *104*, 116029. https://doi.org/10.1103/PhysRevD.104.116029.
35. Giron, J.F.; Lebed, R.F. Simple spectrum of $c\bar{c}c\bar{c}$ states in the dynamical diquark model. *Phys. Rev. D* **2020**, *102*, 074003. https://doi.org/10.1103/PhysRevD.102.074003.
36. Karliner, M.; Rosner, J.L. Interpretation of structure in the di-J/ψ spectrum. *Phys. Rev. D* **2020**, *102*, 114039. https://doi.org/10.1103/PhysRevD.102.114039.
37. Zhao, Z.; Xu, K.; Kaewsnod, A.; Liu, X.; Limphirat, A.; Yan, Y. Study of charmoniumlike and fully-charm tetraquark spectroscopy. *Phys. Rev. D* **2021**, *103*, 116027. https://doi.org/10.1103/PhysRevD.103.116027.
38. Mutuk, H. Nonrelativistic treatment of fully-heavy tetraquarks as diquark-antidiquark states. *Eur. Phys. J. C* **2021**, *81*, 367. https://doi.org/10.1140/epjc/s10052-021-09176-8.
39. Wang, G.J.; Meng, L.; Oka, M.; Zhu, S.L. Higher fully charmed tetraquarks: Radial excitations and P-wave states. *Phys. Rev. D* **2021**, *104*, 036016. https://doi.org/10.1103/PhysRevD.104.036016.
40. Wang, Z.G. Tetraquark candidates in the LHCb's di-J/ψ mass spectrum. *Chin. Phys. C* **2020**, *44*, 113106. https://doi.org/10.1088/1674-1137/abb080.
41. Ke, H.W.; Han, X.; Liu, X.H.; Shi, Y.L. Tetraquark state $X(6900)$ and the interaction between diquark and antidiquark. *Eur. Phys. J. C* **2021**, *81*, 427. https://doi.org/10.1140/epjc/s10052-021-09229-y.

42. Zhu, R. Fully-heavy tetraquark spectra and production at hadron colliders. *Nucl. Phys. B* **2021**, *966*, 115393. https://doi.org/10.1016/j.nuclphysb.2021.115393.
43. Jin, X.; Xue, Y.; Huang, H.; Ping, J. Full-heavy tetraquarks in constituent quark models. *Eur. Phys. J. C* **2020**, *80*, 1083. https://doi.org/10.1140/epjc/s10052-020-08650-z.
44. Yang, G.; Ping, J.; Segovia, J. Exotic resonances of fully-heavy tetraquarks in a lattice-QCD insipired quark model. *Phys. Rev. D* **2021**, *104*, 014006. https://doi.org/10.1103/PhysRevD.104.014006.
45. Albuquerque, R.M.; Narison, S.; Rabemananjara, A.; Rabetiarivony, D.; Randriamanatrika, G. Doubly-hidden scalar heavy molecules and tetraquarks states from QCD at NLO. *Phys. Rev. D* **2020**, *102*, 094001. https://doi.org/10.1103/PhysRevD.102.094001.
46. Albuquerque, R.M.; Narison, S.; Rabetiarivony, D.; Randriamanatrika, G. Doubly hidden 0^{++} molecules and tetraquarks states from QCD at NLO. *Nucl. Part. Phys. Proc.* **2021**, *312-317*, 15289. https://doi.org/10.1016/j.nuclphysbps.2021.05.031.
47. Wu, R.H.; Zuo, Y.S.; Wang, C.Y.; Meng, C.; Ma, Y.Q.; Chao, K.T. NLO results with operator mixing for fully heavy tetraquarks in QCD sum rules **2022**, arXiv:hep-ph/2201.11714.
48. Asadi, Z.; Boroun, G.R. Masses of fully heavy tetraquark states from a four-quark static potential model. *Phys. Rev. D* **2022**, *105*, 014006. https://doi.org/10.1103/PhysRevD.105.014006.
49. Yang, B.C.; Tang, L.; Qiao, C.F. Scalar fully-heavy tetraquark states $QQ'\bar{Q}\bar{Q}'$ in QCD sum rules. *Eur. Phys. J. C* **2021**, *81*, 324. https://doi.org/10.1140/epjc/s10052-021-09096-7.
50. Feng, F.; Huang, Y.; Jia, Y.; Sang, W.L.; Xiong, X.; Zhang, J.Y. Fragmentation production of fully-charmed tetraquarks at LHC **2020**, arXiv:hep-ph/2009.08450.
51. Ma, Y.Q.; Zhang, H.F. Exploring the Di-J/ψ Resonances around 6.9 GeV Based on *ab initio* Perturbative QCD. *arXiv* **2020**, arXiv:hep-ph/2009.08376.
52. Maciuła, R.; Schäfer, W.; Szczurek, A. On the mechanism of $T_{4c}(6900)$ tetraquark production. *Phys. Lett. B* **2021**, *812*, 136010. https://doi.org/10.1016/j.physletb.2020.136010.
53. Gonçalves, V.P.; Moreira, B.D. Fully-heavy tetraquark production by $\gamma\gamma$ interactions in hadronic collisions at the LHC. *Phys. Lett. B* **2021**, *816*, 136249. https://doi.org/10.1016/j.physletb.2021.136249.
54. Wang, X.Y.; Lin, Q.Y.; Xu, H.; Xie, Y.P.; Huang, Y.; Chen, X. Discovery potential for the LHCb fully-charm tetraquark $X(6900)$ state via $\bar{p}p$ annihilation reaction. *Phys. Rev. D* **2020**, *102*, 116014. https://doi.org/10.1103/PhysRevD.102.116014.
55. Esposito, A.; Manzari, C.A.; Pilloni, A.; Polosa, A.D. Hunting for tetraquarks in ultraperipheral heavy ion collisions. *Phys. Rev. D* **2021**, *104*, 114029. https://doi.org/10.1103/PhysRevD.104.114029.
56. Zhuang, Z.; Zhang, Y.; Ma, Y.; Wang, Q. The lineshape of the compact fully heavy tetraquark. *arXiv* **2021**, arXiv:hep-ph/2111.14028.
57. Zhao, J.; Shi, S.; Zhuang, P. Fully-heavy tetraquarks in a strongly interacting medium. *Phys. Rev. D* **2020**, *102*, 114001. https://doi.org/10.1103/PhysRevD.102.114001.
58. Becchi, C.; Ferretti, J.; Giachino, A.; Maiani, L.; Santopinto, E. A study of $cc\bar{c}\bar{c}$ tetraquark decays in 4 muons and in $D^{(*)}\bar{D}^{(*)}$ at LHC. *Phys. Lett. B* **2020**, *811*, 135952. https://doi.org/10.1016/j.physletb.2020.135952.
59. Sonnenschein, J.; Weissman, D. Deciphering the recently discovered tetraquark candidates around 6.9 GeV. *Eur. Phys. J. C* **2021**, *81*, 25. https://doi.org/10.1140/epjc/s10052-020-08818-7.
60. Zhu, J.W.; Guo, X.D.; Zhang, R.Y.; Ma, W.G.; Li, X.Q. A possible interpretation for $X(6900)$ observed in four-muon final state by LHCb – A light Higgs-like boson? *arXiv* **2020**, arXiv:hep-ph/2011.07799.
61. Wan, B.D.; Qiao, C.F. Gluonic tetracharm configuration of $X(6900)$. *Phys. Lett. B* **2021**, *817*, 136339. https://doi.org/10.1016/j.physletb.2021.136339.
62. Gordillo, M.C.; De Soto, F.; Segovia, J. Diffusion Monte Carlo calculations of fully-heavy multiquark bound states. *Phys. Rev. D* **2020**, *102*, 114007. https://doi.org/10.1103/PhysRevD.102.114007.
63. Liu, M.Z.; Geng, L.S. Is $X(7200)$ the heavy anti-quark diquark symmetry partner of $X(3872)$? *Eur. Phys. J. C* **2021**, *81*, 179. https://doi.org/10.1140/epjc/s10052-021-08980-6.
64. Majarshin, A.J.; Luo, Y.A.; Pan, F.; Segovia, J. Bosonic algebraic approach applied to the [QQ][Q¯Q¯] tetraquarks. *Phys. Rev. D* **2022**, *105*, 054024. https://doi.org/10.1103/PhysRevD.105.054024.
65. Kuang, Z.; Serafin, K.; Zhao, X.; Vary, J.P. All-charm tetraquark in front form dynamics. *Phys. Rev. D* **2022**, *105*, 094028. https://doi.org/10.1103/PhysRevD.105.094028.
66. Wang, Q.N.; Yang, Z.Y.; Chen, W. Exotic fully-heavy $Q\bar{Q}Q\bar{Q}$ tetraquark states in $\mathbf{8}_{[Q\bar{Q}]} \otimes \mathbf{8}_{[Q\bar{Q}]}$ color configuration. *Phys. Rev. D* **2021**, *104*, 114037. https://doi.org/10.1103/PhysRevD.104.114037.
67. Chen, W.; Chen, H.X.; Liu, X.; Steele, T.G.; Zhu, S.L. Hunting for exotic doubly hidden-charm/bottom tetraquark states. *Phys. Lett. B* **2017**, *773*, 247–251. https://doi.org/10.1016/j.physletb.2017.08.034.
68. Czarnecki, A.; Leng, B.; Voloshin, M.B. Stability of tetrons. *Phys. Lett. B* **2018**, *778*, 233–238. https://doi.org/10.1016/j.physletb.2018.01.034.

69. Guo, Z.H.; Oller, J.A. Insights into the inner structures of the fully charmed tetraquark state $X(6900)$. *Phys. Rev. D* **2021**, *103*, 034024. https://doi.org/10.1103/PhysRevD.103.034024.
70. Cao, Q.F.; Chen, H.; Qi, H.R.; Zheng, H.Q. Some remarks on $X(6900)$. *Chin. Phys. C* **2021**, *45*, 103102. https://doi.org/10.1088/1674-1137/ac0ee5.
71. Gong, C.; Du, M.C.; Zhao, Q.; Zhong, X.H.; Zhou, B. Nature of $X(6900)$ and its production mechanism at LHCb. *Phys. Lett. B* **2022**, *824*, 136794. https://doi.org/10.1016/j.physletb.2021.136794.
72. Dong, X.K.; Baru, V.; Guo, F.K.; Hanhart, C.; Nefediev, A.; Zou, B.S. Is the existence of a $J/\psi J/\psi$ bound state plausible? *Sci. Bull.* **2021**, *66*, 1577. https://doi.org/10.1016/j.scib.2021.09.009.
73. Ortega, P.G.; Entem, D.R.; Fernández, F. Exploring T$\psi\psi$ tetraquark candidates in a coupled-channels formalism. *Phys. Rev. D* **2023**, *108*, 094023. https://doi.org/10.1103/PhysRevD.108.094023.
74. Wang, G.J.; Meng, Q.; Oka, M. S-wave fully charmed tetraquark resonant states. *Phys. Rev. D* **2022**, *106*, 096005. https://doi.org/10.1103/PhysRevD.106.096005.
75. Zhou, Q.; Guo, D.; Kuang, S.Q.; Yang, Q.H.; Dai, L.Y. Nature of the X(6900) in partial wave decomposition of J/ψJ/ψ scattering. *Phys. Rev. D* **2022**, *106*, L111502. https://doi.org/10.1103/PhysRevD.106.L111502.
76. Liu, W.Y.; Chen, H.X. Fully-heavy hadronic molecules $B_c^{(*)+}B_c^{(*)-}$ bound by fully-heavy mesons **2023**, arXiv:hep-ph/2312.11212.
77. Bando, M.; Kugo, T.; Yamawaki, K. Nonlinear Realization and Hidden Local Symmetries. *Phys. Rept.* **1988**, *164*, 217–314. https://doi.org/10.1016/0370-1573(88)90019-1.
78. Meissner, U.G. Low-Energy Hadron Physics from Effective Chiral Lagrangians with Vector Mesons. *Phys. Rept.* **1988**, *161*, 213. https://doi.org/10.1016/0370-1573(88)90090-7.
79. Oset, E.; Ramos, A. Dynamically generated resonances from the vector octet-baryon octet interaction. *Eur. Phys. J. A* **2010**, *44*, 445–454. https://doi.org/10.1140/epja/i2010-10957-3.
80. Aceti, F.; Bayar, M.; Oset, E.; Martinez Torres, A.; Khemchandani, K.P.; Dias, J.M.; Navarra, F.S.; Nielsen, M. Prediction of an $I = 1$ $D\bar{D}^*$ state and relationship to the claimed $Z_c(3900)$, $Z_c(3885)$. *Phys. Rev. D* **2014**, *90*, 016003. https://doi.org/10.1103/PhysRevD.90.016003.
81. Geng, L.S.; Oset, E. Vector meson-vector meson interaction in a hidden gauge unitary approach. *Phys. Rev. D* **2009**, *79*, 074009. https://doi.org/10.1103/PhysRevD.79.074009.
82. Nagahiro, H.; Roca, L.; Hosaka, A.; Oset, E. Hidden gauge formalism for the radiative decays of axial-vector mesons. *Phys. Rev. D* **2009**, *79*, 014015. https://doi.org/10.1103/PhysRevD.79.014015.
83. Molina, R.; Oset, E. The Y(3940), Z(3930) and the X(4160) as dynamically generated resonances from the vector-vector interaction. *Phys. Rev. D* **2009**, *80*, 114013. https://doi.org/10.1103/PhysRevD.80.114013.
84. Workman, R.L. et al. [Particle Data Group]. Review of Particle Physics. *PTEP* **2022**, *2022*, 083C01. https://doi.org/10.1093/ptep/ptac097.
85. Bečirević, D.; Duplančić, G.; Klajn, B.; Melić, B.; Sanfilippo, F. Lattice QCD and QCD sum rule determination of the decay constants of η_c, J/ψ and h_c states. *Nucl. Phys. B* **2014**, *883*, 306–327. https://doi.org/10.1016/j.nuclphysb.2014.03.024.
86. Mathur, N.; Padmanath, M.; Mondal, S. Precise predictions of charmed-bottom hadrons from lattice QCD. *Phys. Rev. Lett.* **2018**, *121*, 202002. https://doi.org/10.1103/PhysRevLett.121.202002.
87. McNeile, C.; Davies, C.T.H.; Follana, E.; Hornbostel, K.; Lepage, G.P. Heavy meson masses and decay constants from relativistic heavy quarks in full lattice QCD. *Phys. Rev. D* **2012**, *86*, 074503. https://doi.org/10.1103/PhysRevD.86.074503.
88. Aceti, F.; Bayar, M.; Dias, J.M.; Oset, E. Prediction of a $Z_c(4000)$ $D^*\bar{D}^*$ state and relationship to the claimed $Z_c(4025)$. *Eur. Phys. J. A* **2014**, *50*, 103. https://doi.org/10.1140/epja/i2014-14103-1.
89. Oset, E.; Roca, L. Exotic molecular meson states of $B^{(*)}K^{(*)}$ nature. *Eur. Phys. J. C* **2022**, *82*, 882. Erratum: *Eur. Phys. J. C* **2022**, *82*, 1014. https://doi.org/10.1140/epjc/s10052-022-10850-8.
90. Yu, Q.X.; Pavao, R.; Debastiani, V.R.; Oset, E. Description of the Ξ_c and Ξ_b states as molecular states. *Eur. Phys. J. C* **2019**, *79*, 167. https://doi.org/10.1140/epjc/s10052-019-6665-z.
91. Lu, J.X.; Zhou, Y.; Chen, H.X.; Xie, J.J.; Geng, L.S. Dynamically generated $J^P = 1/2^-(3/2^-)$ singly charmed and bottom heavy baryons. *Phys. Rev. D* **2015**, *92*, 014036. https://doi.org/10.1103/PhysRevD.92.014036.
92. Ozpineci, A.; Xiao, C.W.; Oset, E. Hidden beauty molecules within the local hidden gauge approach and heavy quark spin symmetry. *Phys. Rev. D* **2013**, *88*, 034018. https://doi.org/10.1103/PhysRevD.88.034018. L

Disclaimer/Publisher's Note: The statements, opinions and data contained in all publications are solely those of the individual author(s) and contributor(s) and not of MDPI and/or the editor(s). MDPI and/or the editor(s) disclaim responsibility for any injury to people or property resulting from any ideas, methods, instructions or products referred to in the content.